

# Automated Anatomical Labeling of the Bronchial Branch and Its Application to the Virtual Bronchoscopy System

Kensaku Mori\*, Jun-ichi Hasegawa, *Member, IEEE*, Yasuhito Suenaga, and Jun-ichiro Toriwaki, *Senior Member, IEEE*

**Abstract**—This paper describes a method for the automated anatomical labeling of the bronchial branch extracted from a three-dimensional (3-D) chest X-ray CT image and its application to a virtual bronchoscopy system (VBS). Automated anatomical labeling is necessary for implementing an advanced computer-aided diagnosis system of 3-D medical images. This method performs the anatomical labeling of the bronchial branch using the knowledge base of the bronchial branch name. The knowledge base holds information on the bronchial branch as a set of rules for its anatomical labeling. A bronchus region is automatically extracted from a given 3-D CT image. A tree structure representing the essential structure of the extracted bronchus is recognized from the bronchus region. Anatomical labeling is performed by comparing this tree structure of the bronchus with the knowledge base. As an application, we implemented the function to automatically present the anatomical names of the branches that are shown in the currently rendered image in real time on the VBS. The result showed that the method could segment about 57% of the branches from CT images and extracted a tree structure of about 91% in branches in the segmented bronchus. The anatomical labeling method could assign the correct branch name to about 93% of the branches in the extracted tree structure. Anatomical names were appropriately displayed in the endoscopic view.

**Index Terms**—Anatomical labeling, bronchial branch, bronchus, knowledge-based processing, 3-D chest X-ray CT image, virtual bronchoscopy, virtual endoscopy.

## I. INTRODUCTION

**I**N RECENT years, there has been remarkable progress in the use of three-dimensional (3-D) volumetric scanners in the medical field. 3-D images are currently indispensable in diagnosis and treatment. A new computer-aided diagnosis system for 3-D medical images [we call this an advanced computer-aided diagnosis system (ACADS)] is strongly desired to perform the high-level diagnosis of a 3-D medical image. ACADS should have the following functions: 1) automated recognition

of the organ in a 3-D image; 2) analysis of the extracted regions using knowledge-based processing concerning the human anatomy; and 3) visualization of the recognized results such as a shape, a position, or an anatomical name of the organ.

Many algorithms have been proposed for a variety of medical images. Generally, these algorithms can detect the interested region, such as a region suspected to be abnormal, with reasonable accuracy [1]–[3]. Some algorithms use anatomical knowledge of the region that is expected to be extracted. These types of knowledge-based algorithms involve such information as position, diameter, shape, etc. Introducing a knowledge base is very effective for the extraction of the target region from medical images. However, most techniques using a knowledge base are specialized for the segmentation of each region. For example, Sonaka *et al.* use the anatomical knowledge of the bronchus to extract a bronchus region [4]. This knowledge is specialized for the segmentation of the bronchus area of a dog. Very simple knowledge is used for the segmentation. Generally, medical doctors diagnose medical images using their own anatomical knowledge of the target organ. Their diagnostic rules are constructed by using the anatomical names of the organs. If we expect to achieve a high-level computer-aided diagnosis system for 3-D medical images, the system should recognize the anatomical names of the organ and the parts extracted from input images. If it is possible to assign the correct anatomical name to the target organ, the system will be also able to implement the diagnostic rule described by using anatomical names.

A virtual bronchoscopy system (VBS) is a new advanced method for observing a 3-D chest X-ray CT image [5]–[11]. The user can fly through inside the bronchus in real time on the VBS that we have developed [6], [9]. The VBS is applicable to a variety of applications such as diagnosis, surgical planning, informed consent, education, and training. When the user operates the VBS, finding and perceiving the current observation point and orientations are very important, just as it is in the operation of a real endoscope. The operator of the real bronchoscopy should constantly know the current location and the orientation of the observation during the examination. If the VBS can perform automated labeling of bronchial branches and display the label on the virtual endoscopic view, it will help us understand the current viewing position and orientation. One of the most important advantages of the VBS is that it becomes possible to observe the bronchus from the desired viewpoint and the view direction. Furthermore, the user can freely move around inside the bronchus and quickly jump from one point to another arbitrary point. However, a user of these characteristics often feels

Manuscript received May 8, 1999; revised November 1, 1999. This work was supported in part by the Grants-in-Aid for Scientific Research from the Ministry of Education, and in part by the Grants-in-Aid for Cancer Research from the Ministry of Health and Welfare of Japanese Government, and the Hori Information Promotion Foundation. The Associate Editor responsible for coordinating the review of this paper and recommending its publication was W. Niessen. *As-terisk indicates corresponding author.*

\*K. Mori, Y. Suenaga, and J. Toriwaki are with Graduate School of Engineering, Nagoya University, Furo-cho, Chikusa-ku, Nagoya-shi 464-8603, Japan (e-mail: mori@nuie.nagoya-u.ac.jp; toriwaki@nuie.nagoya-u.ac.jp; suenaga@nuie.nagoya-u.ac.jp).

J. Hasegawa is with School of Computer and Cognitive Sciences, Chukyo University, 101, Tokodachi, Kaizu-cho, Toyota-shi, 470-0348, Japan (e-mail: hasegawa@sccs.chukyo-u.ac.jp).

Publisher Item Identifier S 0278-0062(00)02302-8.

difficulty in understanding where he is and in which direction he is traveling or observing in the bronchus. One of the methods for solving this problem is to present the anatomical names of the bronchial branches that are currently being observed in the virtual bronchoscopic view. This function will become very useful in the VBS, since a physician usually realizes the current observation point and orientation by recalling the anatomical names of the visible parts of an organ.

In this paper, we describe a method for the automated anatomical labeling of the bronchial branches extracted from the 3-D chest X-ray CT image of a patient. As applications of this method, we provide a method for automated display of anatomical names rendered in the VBS. The anatomical name of each branch of the bronchus is assigned by using a set of explicit rules. We construct a knowledge base of the anatomical names of the bronchial branch for automated labeling. The labeling procedure assigns the name of the bronchial branch, which is extracted from a CT image of the individual patient by comparing its tree structure using the knowledge and a graph matching strategy.

There have been no reports on the anatomical labeling of the bronchial branch. Although many researchers have reported on VBS or virtual endoscopy (VE), no one has reported a method for the automated display of anatomical names in the VE. Hoehne *et al.* [12] constructed a computerized atlas of the human body called VOXEL-MAN, but the anatomical name of each organ was manually inputted. The VOXEL-MAN is a sophisticated computerized atlas that can be used as a teaching tool. This system displays a computerized atlas and does not offer an environment where the user can travel through inside of an organ in real time.

In Section II of the paper, we describe the knowledge base developed for automated anatomical labeling. Section III presents a method for anatomical labeling. We present applications of anatomical labeling in Section IV. We show the experimental results of the proposed method and add a brief discussion in Section V.

## II. KNOWLEDGE BASE OF ANATOMICAL NAME OF THE BRONCHIAL BRANCH

The bronchus is an organ that has a tree structure. The anatomical name of each branch is assigned based upon a set of rules explicitly defined using the running direction of a branch, the name of the parent branch, and the position of a branch. We implement this set of rules as a knowledge base.

The knowledge base of the bronchial branch is represented by the frame representation well-known in knowledge engineering [21]. This knowledge base is manually constructed. Fig. 1 shows an example. A frame keeps the knowledge of a bronchial branch. It contains information consisting of a tag name of a branch, the anatomical name, the parent branch name, the position, and the direction. The tag name is the name given to treat a bronchial branch in the computer. The item of anatomical name holds the real anatomical name of a bronchial branch represented as text. Direction is the running direction of a branch that is represented by a vector. The item parent branch indicates the tag name of the parent branch of a target branch. Position shows the loca-

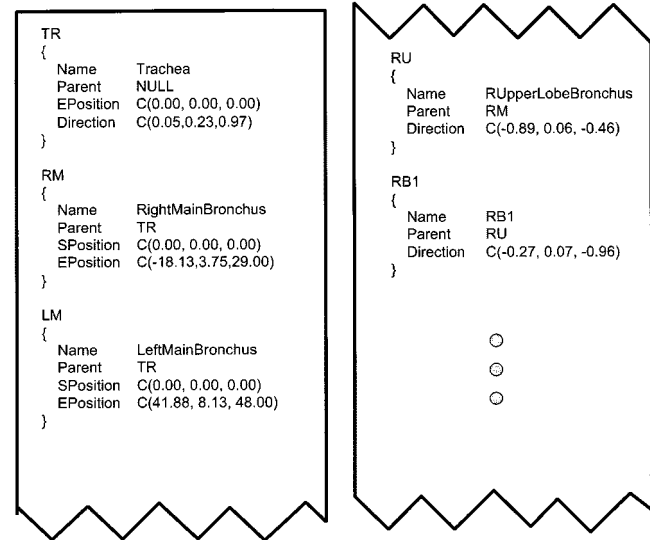


Fig. 1 An example of knowledge base of bronchial branch name. Information on each branch is described as one frame. Each branch is distinguished by a tag name, such as TR, RM, and LM. Only RM and LM have position information. Each branch has information on parent branch name, its running direction.

tion of a bronchial branch. This position is represented by the coordinate system whose origin is at a branching point of the trachea, the  $x$  axis is the coronal direction of the human body, the  $y$  axis is sagittal, and the  $z$ -axis is axial, respectively. Only the left main bronchus (LM) and the right main bronchus (RM) have the position information. Since such information of the peripheral branches is very sensitive for each patient, we only use position information for RM and LM. There is variation in the branching structure among humans. Although we must prepare multiple knowledge bases or a single variable/adaptive knowledge base to treat such variation, we presently use only one knowledge base for a typical branching structure. It is easy to extend knowledge base to one that covers a variety of information on the bronchus. The knowledge is loaded on the computer when the automated labeling procedure is executed. The procedure reads the knowledge represented by the frame, and stores the following information concerning a branch.

*Information of the  $i$ th Branch  $K_i$  in the Knowledge Base:*

index number:  $i$ ;  
 index number of the parent branch:  $p^{K_i}$ ;  
 number of child branches:  $n_c^{K_i}$ ;  
 index numbers of child branches:  $c_1^{K_i}, \dots, c_{n_c^{K_i}}^{K_i}$ ;  
 starting point:  $S^{K_i}$  (only for RM and LM);  
 end point:  $Q^{K_i}$  (only for RM and LM);  
 running direction:  $d^{K_i}$  (for all branches except for RM and LM);  
 anatomical name: "anatomical name."

## III. AUTOMATED LABELING OF THE BRONCHIAL BRANCH

### A. Overview of the Procedure

Fig. 2 shows the complete procedure of automated labeling of the bronchial branch. We assume here that a 3-D chest X-ray CT

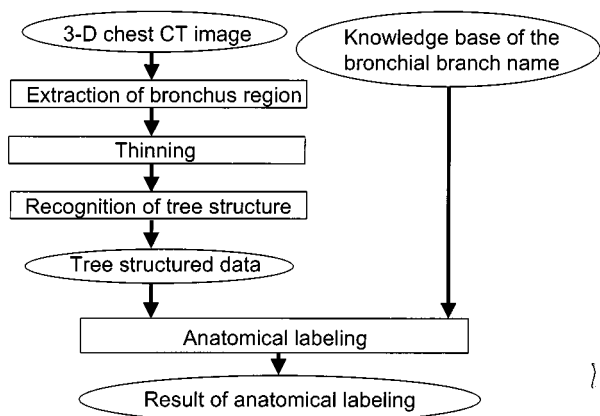


Fig. 2. Procedure for automated anatomical labeling.

image contains the trachea and that the slice thickness and the reconstruction pitch are small enough ( $<5$  mm), we also assume that both the left and right lungs are contained in the image. Although a CT image usually does not have isoresolution for each axis direction, this method uses no interpolation. Unisometric cases are taken into consideration in the calculation of the distance between two voxels.

First, we extract the bronchus region from a 3-D X-ray CT image. The inside region of the bronchus or the airway is extracted by employing a 3-D region-growing algorithm [14]. We extract the air spaces inside the bronchus as the bronchus areas instead of extracting the wall of the bronchus as a curved surface. We perform this by sequentially tracing voxels with relatively low CT values corresponding to the air, starting at a suitable initial voxel. This procedure is based on the simple fact that the bronchus area (the space inside the bronchus) is simply connected. A few methods for extracting the bronchus region from 3-D X-ray CT images have been reported [4],[13]. Compared to these methods, our method is much simpler and still can extract the bronchus region of the sixth branching level in the best case, and that of the third level in the worst case. More details of the method were presented in [14]. The tree structure of the extracted bronchus is recognized from a thinned result of the bronchus region by employing a thinning method [15]. A graph representation that holds the connection relation between each voxel of the thinned result is created. Anatomical labeling of the bronchial branch is performed by comparing the tree structure of the extracted bronchus with the knowledge base using graph matching procedure.

This procedure assumes that both lungs are contained in the CT image. The zoom rate and the rotation angle of the axial directions are assumed to be fixed in the patient. We exclude the cases when an input image has only one side of the lung, or the center of the image is located far from the center of the human body, as both cases are very rare.

## B. Details of the Processing Procedure

### 1) Extraction of the Bronchus Region from a 3-D Chest X-ray CT Image:

a) *Selection of a start point:* An inside point of the trachea is used as the starting point, because the trachea has

very high contrast on a slice and is located at a fixed position. Since the CT values inside the trachea are lower than those surrounding it in chest X-ray CT images, the trachea area is easily extracted by thresholding. CT images start from the slice that contains the trachea part. The center point of each slice corresponds to the center of the human body. The area inside a cross section of the trachea takes CT values of a limited range, because the inside of the trachea is filled with air. The trachea also exists around the center of the human body. Its diameter is typically 20 mm in Japanese adults. Therefore, the trachea is easily extracted from the top slice of an input X-ray CT image. First, the top slice is binarized by thresholding with the threshold value  $t_{\text{trachea}}$  ( $-900$  H.U.). Second, the method selects a connected component  $C$  that satisfies the conditions of the experiment  $t_{\text{area1}} < C_{\text{area}} < t_{\text{area2}}$ , and  $P_{\text{mid}} - P_{\text{mar}} < P_C < P_{\text{mid}} + P_{\text{mar}}$ .<sup>1</sup> Here  $C_{\text{area}}$  means the area of the component  $C$ ,  $t_{\text{area1}}$  and  $t_{\text{area2}}$  are threshold values for the area,  $P_C$  a location of the center of the gravity of  $C$ ,  $P_{\text{mid}}$  the center position of a slice, and  $P_{\text{mar}}$  defines the region where the trachea should exist. These threshold values are fixed for all input images. If more than one component satisfies this condition, we select the one with the largest area. A point with the minimum CT value is used as a starting point of the labeling.

b) *Repetitive region growing:* A kind of 3-D region growing method 3-D painting algorithm is used to extract the bronchus area [14]. This algorithm paints all voxels that have lower CT values. The lower CT values correspond to the air and are connected to each other. This procedure is performed sequentially and starts at the initial point selected inside the trachea as just described. The algorithm extends the colored area to a voxel adjacent to the current voxel and satisfies the specified merging condition. If a visited voxel has a CT value lower than a threshold  $t$ , which distinguishes the inside or outside of the bronchus, then it is recognized as inside the bronchus and assigned a prespecified mark. This painting algorithm is performed with a line-by-line mode along three axes in 3-D space to reduce the computation time. Details are given in reference [14].

c) *Optimization of the threshold value:* An optimization of the threshold value  $t$  is required in the 3-D painting algorithm. This threshold value distinguishes the bronchus wall area from the inside of the bronchus. A threshold value as high as possible is desirable for extracting a bronchus region with the minimum number of false-negative areas. If the threshold value is too high, however, the extracted region will grow over the bronchus wall. In this case the whole or almost all of the lung area may be extracted as the bronchus area in the worst case (we call this case an explosion). The number of extracted voxels will become much larger than that of a normally extracted bronchus area, because the lung area is much larger than the bronchus area. By using this feature, we desire the following painting procedure with optimized thresholding.

The initial painting is performed using a relatively low threshold value and the number of voxels extracted as the

<sup>1</sup>Defining as  $A = (p, q)^T$ ,  $B = (r, s)^T$ , a notation  $A < B$  means that both  $p < r$  and  $q < s$  hold.

bronchus area are counted. Then the painting and counting are iterated with the threshold value increased by an increment of 1 H.U. When the number of extracted voxels exceeds the area threshold value  $t_{\text{area}3}$  (explosion), the iteration is terminated. We regard the result just before this explosion as the desired bronchus area. However, since a sequential scanning for the optimum threshold value takes a great deal of computation time, we employ the well-known binary search method to find an optimum threshold value. Details are given in [14].

2) *Extraction of Branching Structure of the Bronchus:*

a) *Extraction of the medial axis of the bronchus:* The extracted bronchus region is represented by a set of voxels. A medial axis of the bronchus is extracted from the bronchus region by applying the 3-D thinning method, which is augmented with the Euclidean distance transformation [15]. We also apply the Euclidean distance transformation to the extracted bronchus region [16]. Each voxel of the thinned figure has a distance value at the corresponding location in the distance-transformed image. A result of distance transformation is used to eliminate false-positive branches (FPB's) in the next step of the procedure.

b) *Extraction of a tree structure of the bronchus:* We extract the tree structure of the bronchus from the thinned result. This is one of the main parts of labeling since it depends on the tree information of the extracted bronchus. First, the graph representation is derived from the thinned result. This graph represents connections between voxels. Each voxel of the thinned line figure corresponds to a node in this graph [Fig. 3(a)]. The arc of the graph represents the connection between voxels. Each node has the information of its position, the nodes connected to it, and the path to the connected nodes on the thinned result. Second, a node is classified into three types: 1) a branching point (more than two connected arcs); 2) a connecting point (exactly two connected arcs); and 3) a terminating point (only one connected arc). The method deletes all of the connecting points of the graph [Fig. 3(b)]. The result may have a small loop at a branching point, as shown in Fig. 3(c). This loop consists of three small edges whose lengths are a 1-voxel distance in 26 connectivity. Small loops are detected and deleted by in a simple procedure. Details of it are omitted here. Finally, we obtain the branching points and the terminating points in the graph. The tree structure of the bronchus can be easily recognized from these points. A node means a branching point of the bronchial branches, and an arc corresponds to a bronchial branch.

We delete FPB's that are generated by the thinning method due to its side effect. Fig. 4 shows examples of FPB's. An FPB often appears at a branch with a relatively large diameter such as the trachea, the left main bronchus, or the right main bronchus. An FPB is defined here as a branch whose length is shorter than a given threshold value  $t_{\text{length}}$ , or a branch that starts from a branch with a large diameter. Both types of FPB's should satisfy the condition that they have no child branches. A large diameter branch is defined here as a branch whose diameter is larger than a given threshold value  $t_{\text{diameter}}$ . This diameter is calculated by referring to the distance-transformed image obtained in Section III-B2a). The average value of the distance transformed image along the thinned result of the branch is used as a diameter. We delete all branches that satisfy one of the above con-

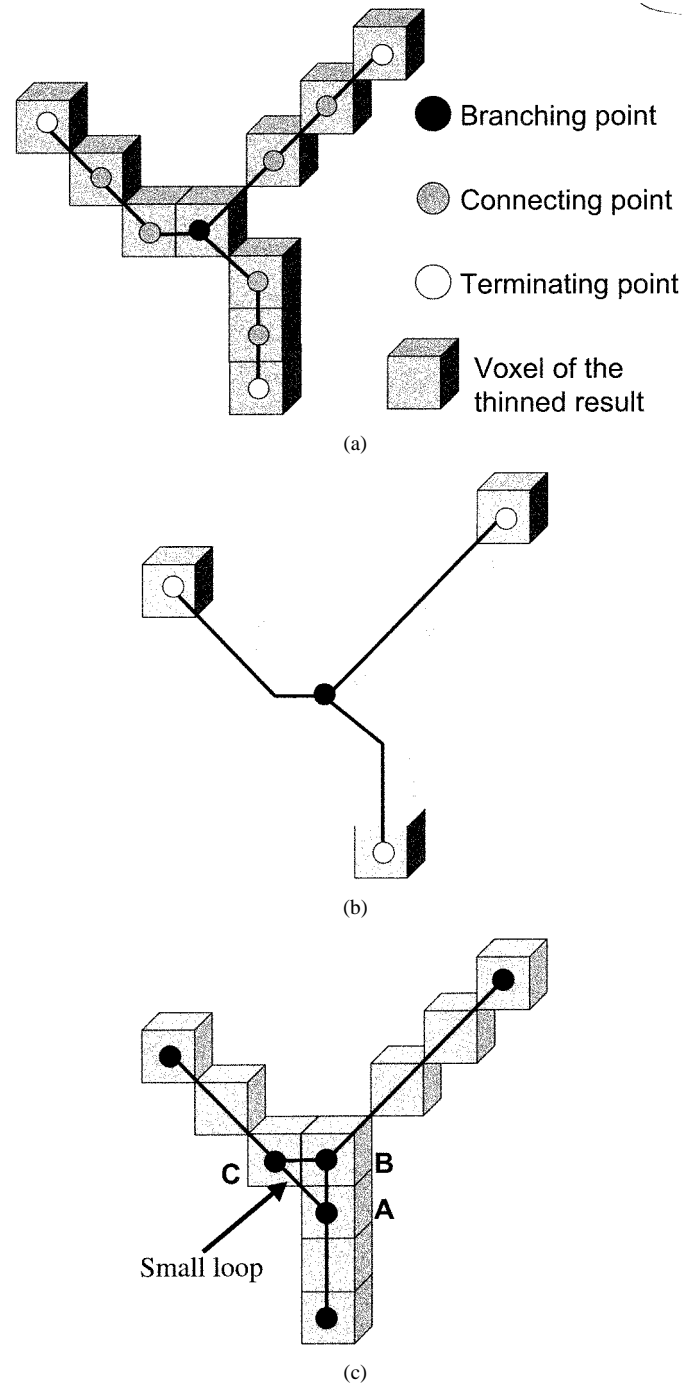


Fig. 3. Graph representation for extracting tree structure from thinned result. (a) Three types of nodes. Each voxel of thinned result is initially considered as the node. Arc of graph connects neighboring nodes in 26 connectivity. Each node is classified into three types, branching point, connecting point, and terminating point. (b) Deletion of all connecting nodes from graph. Each branch is recognized as branch connecting two nodes and also holds information on the path of the thinned result (a set of voxels). (c) Small loop at branching point. Length of edge is just 1-voxel distance in 26 connectivity.

ditions. The threshold values  $t_{\text{length}}$ , and  $t_{\text{diameter}}$  are experimentally determined. When three branches are very close to each other (within 1 voxel), the tree structure at such part is described as the trifurcation structure (a branching point to which four branches connect), or two points as the bifurcation structure. Our knowledge base only supports the bifurcation structure. The labeling may fail if the trifurcation structure appears.

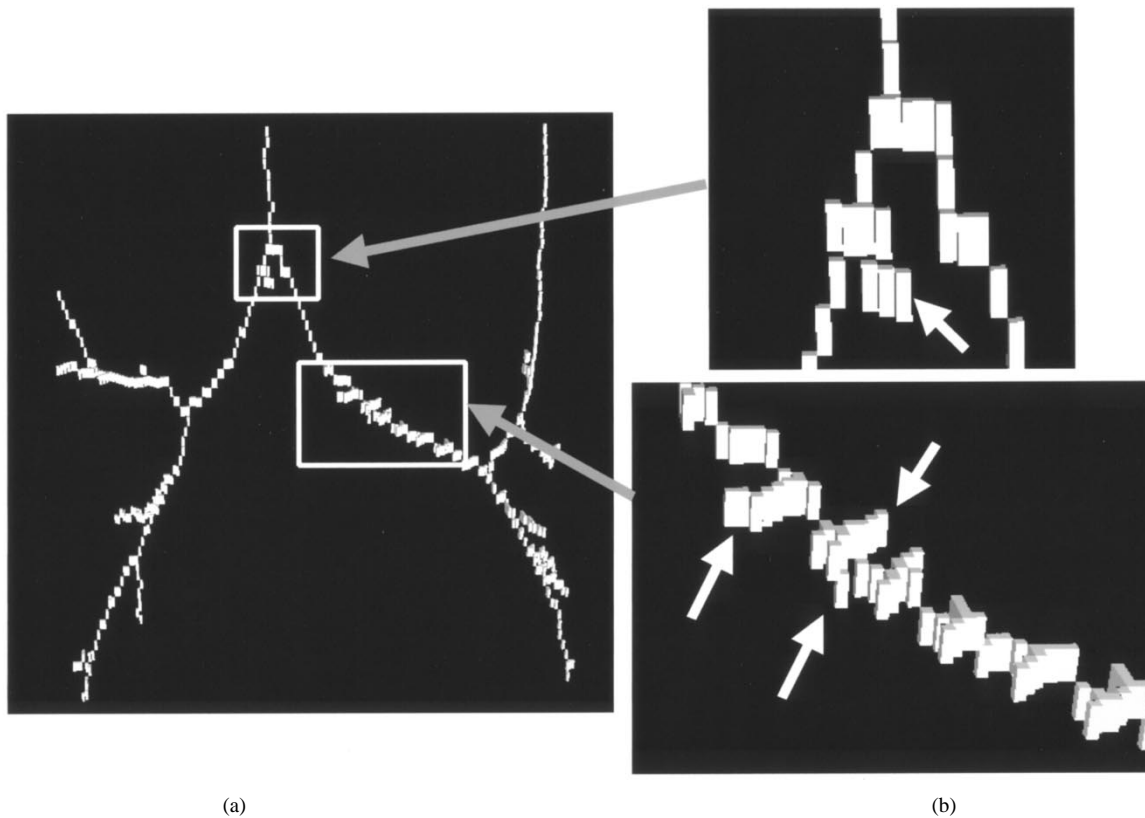


Fig. 4. Examples of FPB's caused by thinned method. (a) Thinned result of bronchus region where each voxel is rendered as a cube. Many FPB's are existing at large branch in right main bronchus and left main bronchus. (b) Magnified views of left side image. FPB's are indicated by arrows.

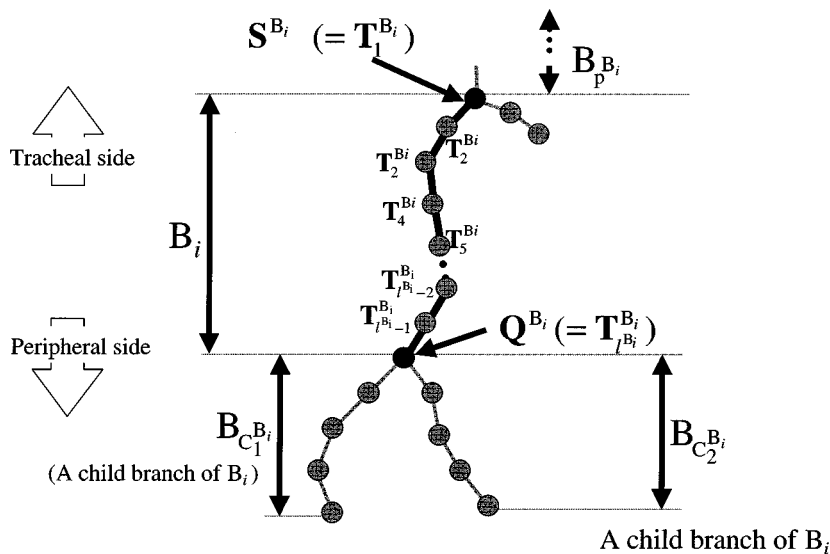


Fig. 5. Information on the  $i$ th branch  $B_i$  of tree structure.

Finally, the information defined in Section II is calculated (Fig. 5). We denote the information of branch  $B_i$  by the superscript  $B_i$ .  $\mathbf{T}^{B_i}$  and  $l^{B_i}$  are also calculated where  $\mathbf{T}^{B_i}$  is a thinned result of  $B_i$  and  $l^{B_i}$  is its length.  $\mathbf{T}^{B_i}$  is then defined as a set of voxels

$$\mathbf{T}^{B_i} = \{\mathbf{T}_1^{B_i}, \dots, \mathbf{T}_{l^{B_i}}^{B_i} \mid \mathbf{T}_m^{B_i} = (x_m^{B_i}, y_m^{B_i}, z_m^{B_i}), 1 \leq m \leq l^{B_i}\} \quad (1)$$

where  $\mathbf{T}_m^{B_i}$  is the position of the  $m$ th voxel of the thinned result of branch  $B_i$ .  $\mathbf{T}_1^{B_i}$  is located at the center of the human body, and  $\mathbf{T}_{l^{B_i}}^{B_i}$  is at a peripheral side.

3) *Automated Anatomical Labeling of the Bronchial Branch*: The procedure for anatomical labeling consists of two parts: a) finding main bronchi (RM: right main bronchus, LM: left main bronchus) and b) anatomical labeling of peripheral bronchial branches (except for the trachea, the RM and the LM). The RM and the LM exist at almost fixed positions because we

TABLE I  
SPECIFICATION OF CT IMAGES USED IN EXPERIMENT

	Image Size (pixelxpixel)	Number of slices	Pixel Size (mmxmm)	Thickness (mm)	Reconstruction Pitch (mm)
Case001	512x512	62	0.625x0.625	2.0	1.0
Case002	512x512	63	0.625x0.625	2.0	1.0
Case003	512x512	118	0.625x0.625	2.0	1.0
Case004	512x512	101	0.625x0.625	2.0	1.0
Case005	512x512	180	0.625x0.625	2.0	1.0
Case006	512x512	120	0.625x0.625	2.0	1.0
Case007	512x512	148	0.625x0.625	3.0	1.0
Case008	512x512	81	0.625x0.625	5.0	2.0
Case009	512x512	78	0.625x0.625	5.0	2.0
Case010	512x512	79	0.625x0.625	5.0	2.0
Case011	512x512	80	0.625x0.625	5.0	2.0
Case012	512x512	50	0.625x0.625	5.0	2.0
Case013	512x512	82	0.625x0.625	5.0	2.0
Case014	512x512	183	0.625x0.625	5.0	1.0

measure their positions from the trachea. Procedure a) assigns the RM and the LM to branches of the tree structure by using their position information. Some FPB's caused by thinning errors may appear around the RM and the LM, as shown in Fig. 4. All branches are child branches of the RM or the LM. If the labeling fails at these branches, it fails in labeling all branches of the bronchus. To avoid this, we employ a particular procedure that finds them by using position information. In Procedure b), peripheral branches of the RM and the LM are labeled sequentially from the RM and the LM with the depth first search. Here we show the automated anatomical labeling procedure.

a) *Finding the RM and LM*: First the method selects candidate branches  $B_a^i$  ( $i = 1, \dots, n$ ;  $n$  is the number of candidate branches) of the RM that satisfy

$$\|Q^{B_a^i} - Q^{K_{RM}}\| < k \quad (2)$$

from the tree structure. Here  $k$  is a given constant defining a margin of location for an end point of RM,  $Q^{B_a^i}$  an end point of  $B_a^i$ , and  $Q^{K_{RM}}$  the end point of the RM defined in the knowledge base. For each candidate  $B_a^i$ , the labeling of all child branches of  $B_a^i$  is performed by regarding  $B_a^i$  as the RM and using the procedure described in Section III-B3b). We define an evaluation value  $E_a^i$  for  $B_a^i$  as

$$E_a^i = \sum_{\text{for all } B_g \in \{\text{child branches of } B_a^i\}} E_{B_g K_g} \quad (3)$$

where  $B_g$  is a child branch of  $B_a^i$  and  $K_g$  is a branch of the knowledge base assigned to  $B_g$  and defined in (4). The RM is found by selecting the  $B_a^i$  with has the highest  $E_a^i$ . The LM is found in the same way.

b) *Labeling of peripheral branches*: The basic labeling of each branch of the tree structure is executed by selecting the branch  $K_{j \max}$  which maximizes the evaluation value  $E_{B_i K_j}$  and whose parent name is the same as the parent branch name of the target branch from the knowledge base.  $E_{B_i K_j}$  is calculated by

$$E_{B_i K_j} = \frac{\mathbf{d}^{B_i} \cdot \mathbf{d}^{K_j}}{\|\mathbf{d}^{B_i}\| \|\mathbf{d}^{K_j}\|} \quad (4)$$

where  $B_i$  is a labeling target branch and  $K_j$  is one of the branches whose parent names are the same as the parent branch name of  $B_i$ .  $\mathbf{d}^{B_i}$  and  $\mathbf{d}^{K_j}$  are running directions of  $B_i$  and  $K_j$ , respectively. Since we only treat the image where the zoom ratio and the axial rotation of the patient are fixed among all cases, we can directly use the running direction information in the knowledge base. We assign the anatomical name of the selected branch to the target branch of the tree structure.

If the selected  $K_{j \max}$  was already assigned to another branch  $B_b$ , we compare the evaluation values  $E_{B_i K_{j \max}}$  and  $E_{B_b K_{j \max}}$ . If  $E_{B_i K_{j \max}} > E_{B_b K_{j \max}}$ , the branch name of  $K_{j \max}$  is then assigned to  $B_i$  and the old label of  $B_b$  and its child are canceled. Otherwise, the second branch is assigned to  $B_i$ . This process avoids assigning the same label to different branches. The parent name of the target branch should be the same parent branch name as that in the knowledge base. Since the cancellation in the branch name may cause inconsistency in the parent branch name, the method also cancels the names of child branches of  $B_b$  and retries the assignment.

This assignment process is executed from the trachea to the periphery direction with the depth first search. The labeling process is iterated until no assignment can be performed.

#### IV. AUTOMATED DISPLAY OF THE ANATOMICAL NAME OF THE BRONCHIAL BRANCH IN THE VBS

Our VBS generates an endoscopic view by rendering a polygonal surface derived from the extracted bronchus region. The viewpoint is located inside the bronchus. The user can interactively specify a viewpoint  $V_p$  and a view direction  $V_d$  and the corresponding endoscopic view is immediately presented on a graphics terminal. We can arbitrarily specify  $V_p$  and  $V_d$ . The automated presentation of anatomical names is performed by selecting branches that are rendered in the virtual endoscopic views, and their anatomical names are overlaid on a rendered image.

The current branch  $B_i$  is determined by calculating the closest branch from the current viewpoint. We define the distance  $R_{B_i V_p}$  between the branch  $B_i$  and the current  $V_p$  by

$$R_{B_i V_p} = \min_{m=1,2,\dots,l^{B_i}} \|\mathbf{T}_m^{B_i} - V_p\| \quad (5)$$

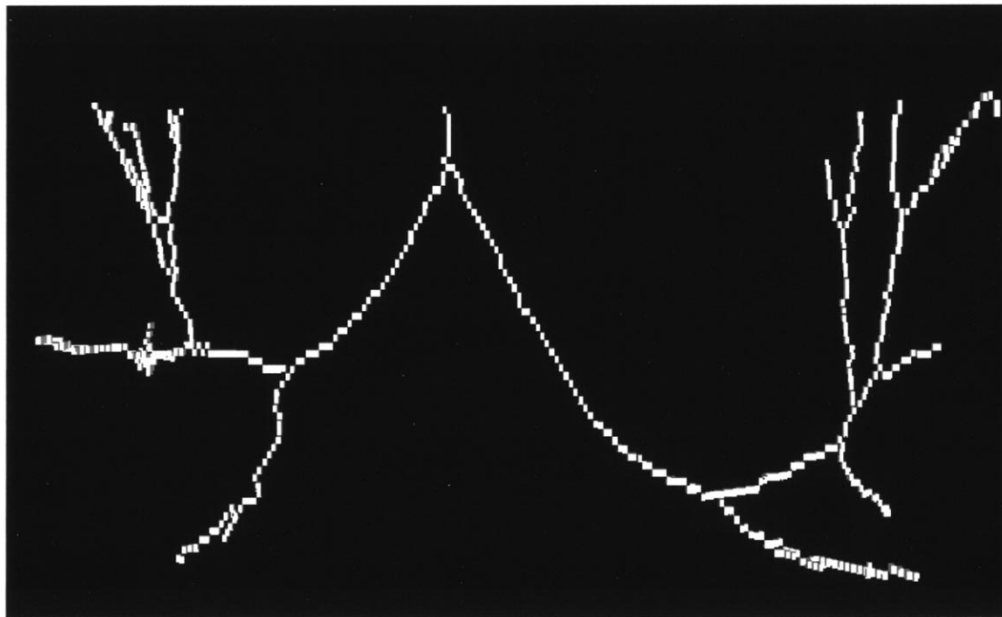
where  $\mathbf{T}_m^{B_i}$  is the  $m$ th point of the path of the branch  $B_i$ ,  $V_p$  is a vector representing the current viewpoint, and  $l^{B_i}$  is the length of the branch  $B_i$ . The closest branch that corresponds to  $V_p$  is found by calculating a branch  $B_i$  that minimizes  $R_{B_i V_p}$  for all branches of the tree structure. The current observation direction (from center to peripheral or from peripheral to center) is also found automatically by using the angle between the current view direction and the direction of the closest branch. The following relation locates the observation direction:

$$\begin{aligned} &\text{observation direction} \\ &= \begin{cases} \text{from center peripheral,} & \text{if } \mathbf{d}^{B_i} \cdot V_d \geq 0 \\ \text{from peripheral center,} & \text{otherwise.} \end{cases} \quad (6) \end{aligned}$$

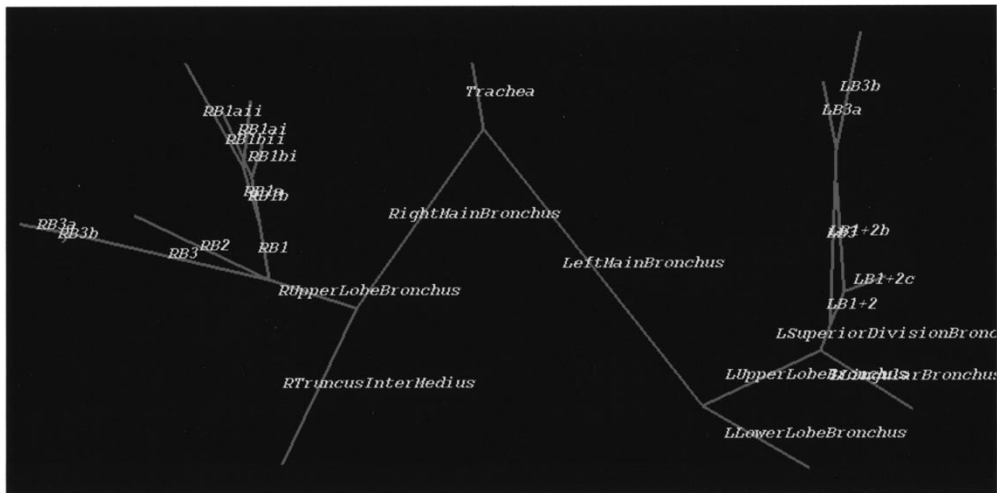
Here  $V_d$  is a vector that means the current view direction in the VBS,  $\mathbf{d}^{B_i}$  is the running direction of branch  $B_i$ .



(a)



(b)



(c)

Fig. 6. A result of automated anatomical labeling of bronchial branch. (a) Extracted region of bronchus. (b) Thinned result of bronchus region. (c) Tree structure extraction and anatomical labeling. Lines show bronchial branches. Anatomical name assigned to branch is displayed at branch by code. All anatomical names are correctly assigned by the method.

When the view direction is from center to peripheral, we select two types of branches,  $B_i$  and  $\{B_{c_1^{B_i}}, \dots, B_{c_{n_c^{B_i}}^{B_i}}\}$ , to display anatomical names.  $B_i$  is the branch in which the current viewpoint  $V_p$  is located and  $\{B_{c_1^{B_i}}, \dots, B_{c_{n_c^{B_i}}^{B_i}}\}$  is a set of the child branches of  $B_i$ . When the view direction is from peripheral to center, we select branches  $B_i$  and  $B_{p^{B_i}}$  to present anatomical names where  $B_{p^{B_i}}$  is the parent branch of  $B_i$ . The anatomical names of the selected branches are displayed at the positions corresponding to the selected branches in the virtual bronchoscopy image. The branch name of the current branch is presented at the lower left corner of the endoscopic view. To display a branch name other than the current branch  $B_i$ , we calculate the 3-D position of the selected branch. Let  $B_j$  be a selected branch for displaying anatomical names. Location  $L^{B_j}$  of branch  $B_j$  is considered as follows:

$$L^{B_j} = \frac{T_1^{B_j} + T_{t^{B_j}}^{B_j}}{2}. \quad (7)$$

Refer to (1) for  $T_1^{B_j}$  and  $T_{t^{B_j}}^{B_j}$  meaning. This formula defines the 3-D location of branch  $B_j$  as the middle point of the line that connects a starting point and an end point of  $B_j$ . The 2-D position for displaying an anatomical name on the endoscopic view is determined by projecting  $L^{B_j}$  onto the projection plane, which is defined by the current viewing parameters of the virtual endoscopic view. When the viewpoint and the view direction are changed, a set of branches with anatomical names is updated. Their positions are also changed.

## V. EXPERIMENTS AND DISCUSSION

### A. Automated Anatomical Labeling of the Bronchial Branch

1) *Experiment:* We applied the method of automated anatomical labeling to fourteen cases of 3-D chest X-ray CT images taken by a helical CT scanner. Table I shows the image specifications. To prepare the database beforehand, we manually inputted the information about the bronchial branches by using textbooks on bronchial anatomy [18–20]. Typical branching structures which are explained in the text book were used to construct the knowledge base. Therefore, the knowledge base does not have any particular relation to the test cases of images used here except for position information of the RM and LM. Positions of the RM and LM are averages of all cases we used in the experiment. We have experimentally determined the threshold values  $t_{\text{area1}}$  ( $= 400 \text{ mm}^2$ ),  $t_{\text{area2}}$  ( $= 80 \text{ mm}^2$ ),  $t_{\text{area3}}$ ,  $t_{\text{length}}$  ( $= 3 \text{ mm}$ ),  $t_{\text{diameter}}$  ( $= 15 \text{ mm}$ ),  $k$  ( $= 15 \text{ mm}$ ),  $P_{\text{margin}}$  ( $= (10 \text{ mm}, 10 \text{ mm})^T$  away from the center point of the slice).  $t_{\text{area3}}$  was selected as the number of slices  $\times 1000$  (voxels) and the other values were fixed for all cases. It was very easy to detect the explosion by using  $t_{\text{area3}}$  in all cases. Fig. 6(a) is an example of the outside views of the bronchus extracted from the CT image. Fig. 6(b) is a thinned result of the extracted bronchus region, and Fig. 6(c) is the tree structure and the assignment result of anatomical names. It took 10 s to extract the bronchus region, 60 s to extract the tree structure, and 5 s for labeling on an SGI Octane MXE R10000 250 MHz.

2) *Validation:* We validated the experimental results by counting the extracted bronchi from CT images, the branches recognized in the recognition process of the tree structure, and the branches whose anatomical names were correctly assigned. We also counted this information in each branching level. We define the branching level of the trachea as the zero level and the RM and the LM as the first level. Table II shows the results. As the difficulty of anatomical labeling increases in proportion to the branching level in the tree structure, we validated the result according to the level in the tree structure. The table also shows the number of the bronchial branches that were recognized in each CT image by the author. We tested two types of images, the thick slice image and thin slice image. The former were taken by 5-mm width of the X-ray beam and the latter 2 mm or 3 mm. Since the recognition rate depends on the thickness of the X-ray beam we evaluated the results separately.

The method extracted 67% of the branches that were observed in the input thin slice CT images by one of the authors Dr. K. Mori who is an experienced observer of chest X-ray CT images. About 85% of branches within the fourth branching level were extracted. The deepest branch was at the sixth level. Its diameter was estimated to be about 1.2 mm on the CT image. This diameter value was estimated on the CT image under the display condition of  $-1050 \text{ H.U.}$  of the window level and  $2100 \text{ H.U.}$  of the window width. For a thick slice image, about 42% of branches were extracted from CT images and 55% were extracted within the fourth level. The lower recognition rate was due to the partial volume effect, which is very strong in thick slice images. CT values inside the branches of the thick slice image became higher than the value of the branch of the thin slice images. The branch that ran parallel to the slice plane was heavily affected. The automated extraction procedure detects the optimum threshold value in order to distinguish the inside or the outside voxel of the bronchus by using an explosion approach. Although this method is very simple, it may not be able to treat any of disease cases such as stenosis or a large tumor.

We could recognize 91% of the branching structures of the extracted bronchi. Approximately 9% of branches were not recognized because the algorithm for the elimination of FPB's erroneously deleted the true positive branches in trading for many successful limitation of FPB's during tree structure extraction. Parameters for the deletion of FPB's were set experimentally. The tradeoff between the elimination of FPB's and false deletion of correct branches is delicate and further parameter adjustment is required. We must also improve the 3-D thinning algorithm or develop of a thinning method that does not result in the FPB's. Different type of methods that may replace the thinning such as the method described in [17].

The third row for each case of the table shows the number of correctly assigned branches. We assigned correct names to 93% of the branches extracted in the stage of obtaining the tree structure. The labeling procedure labeled about 97% of the segmented branches within the fourth level of branching in thin slice images and 91% in thick slice images. This shows that the presented method can assign the correct name to the main branch.

3) *Discussion:* Mistakes were caused by the difference in the branching structures of individual patients and false-positive



TABLE II

RESULT OF EXTRACTION OF BRONCHUS REGION, EXTRACTION OF TREE STRUCTURE AND ANATOMICAL LABELING. (a) THIN SLICE IMAGES. (b) THICK SLICE CT IMAGES. (c) BRANCHES CLASSIFIED INTO EACH BRANCHING LEVEL. ONLY ENUMERATES WITHIN SEGMENTAL BRANCHES AND LEVEL 6 BRANCHING LEVEL DUE TO SPACE LIMITATIONS. THE RESULT IS EVALUATED ACCORDING TO THE NUMBER OF BRANCHES. SEGMENTATION SHOWS NUMBER OF EXTRACTED BRANCHES FROM CT IMAGES AND NUMBER OF BRONCHIAL BRANCHES RECOGNIZED ON CT IMAGES BY AUTHOR. 30/37 MEANS THAT 37 BRANCHES EXISTED IN A CT IMAGE AND 30 BRANCHES WERE EXTRACTED. TREE STRUCTURE SHOWS NUMBER OF BRANCHES RECOGNIZED IN TREE STRUCTURE EXTRACTION. LABELING PRESENTS NUMBER OF BRANCHES WITH CORRECTLY ASSIGNED ANATOMICAL NAMES. RESULTS ARE ALSO CLASSIFIED ACCORDING TO BRANCHING LEVEL. LEVEL  $n$  SHOWS NUMBER OF BRANCHES WITH  $n$ TH BRANCHING LEVEL. TRACHEA IS LOCATED AT ZERO BRANCHING LEVEL. RIGHT AND LEFT MAIN BRONCHI ARE ON FIRST BRANCHING LEVEL. LEVELS USED HERE DO NOT CORRESPOND TO ANATOMICAL BRANCHING LEVEL SUCH AS LOBAR LEVEL OR SEGMENTAL LEVEL

		Total	Level0	Level1	Level2	Level3	Level4	Level5	Level6
Case001	Segmentation	30/37	1/1	2/2	4/4	7/7	6/8	8/9	2/6
	Tree extraction	28	1	2	4	5	6	8	2
	Labeling	28	1	2	4	5	6	8	2
Case002	Segmentation	27/28	1/1	2/2	4/4	4/5	8/8	8/8	0/0
	Tree extraction	25	1	2	4	4	6	8	0
	Labeling	25	1	2	4	4	6	8	0
Case003	Segmentation	47/75	1/1	2/2	4/4	9/9	16/16	13/25	2/18
	Tree extraction	43	1	2	4	9	16	11	0
	Labeling	43	1	2	4	9	16	11	0
Case004	Segmentation	17/20	1/1	2/2	4/4	6/6	2/2	2/5	0/0
	Tree extraction	17	1	2	4	6	2	2	0
	Labeling	17	1	2	4	6	2	2	0
Case005	Segmentation	38/63	1/1	2/2	4/4	7/9	12/18	10/13	2/16
	Tree extraction	31	1	2	4	6	8	8	2
	Labeling	25	1	2	4	6	6	4	2
Case006	Segmentation	22/46	1/1	2/2	4/4	9/9	4/17	2/9	0/4
	Tree extraction	15	1	2	4	4	2	2	0
	Labeling	15	1	2	4	4	2	2	0
Case007	Segmentation	37/51	1/1	2/2	4/4	8/8	13/17	7/15	2/4
	Tree extraction	37	1	2	4	8	13	7	2
	Labeling	32	1	2	4	8	10	5	2
Total	Segmentation	218/320	7/7	14/14	28/28	50/53	61/86	50/84	8/48
	Tree extraction	196	7	14	28	42	53	46	6
	Labeling	185	7	14	28	42	48	40	6
Accumulated	Segmentation	-	7/7	21/21	49/49	99/102	160/188	210/272	218/320
Total	Tree extraction	-	7	21	49	91	144	190	196
	Labeling	-	7	21	49	91	139	179	185

(a)

or false-negative branches in the tree structure extraction. We prepared the knowledge base for only one type of branching structure. One of the patients used in the experiment had a different branching structure. Our model supports only a branching structure where RB1, RB2, and RB3 are separately dividing from the upper main bronchus, and both RB1a and RB1b start from RB1. The mislabeled patient showed RB1a and RB1b starting from RB2 and RB3. In this case, all bronchial branches in the S1 region were labeled as the child branches of RB2 or RB3 (e.g., RB2a, RB2b). These branches should have been labeled as RB1a and RB1b, respectively. One solution to these problems is to prepare different types of the knowledge base to cover different branching structures. In the future, we plan to perform a labeling procedure with several knowledge bases to cover variations. The appropriate knowledge base is the one with the highest sum of the evaluation values.

A false-positive or false-negative branch is also a serious problem in automated labeling. When false-positive or false-negative branches exist in the tree, the branching structure differs from the one in the knowledge base. The proposed method could not correctly treat this case and misassignments

occurred. In the experiment, misrecognition was caused by the lack of RB6 or LB6. The extraction of these branches was very difficult due to the partial volume effect. Our knowledge base assumes that RB6 or LB6 exists. When the extraction of these branches failed, the tree structure lacked the RB6 and the LB6 and the labeling failed for the bronchi of the lower lobe. In addition, the method labeled the FPB as the bronchial branch, so that all children of the branch connected to the FPB were labeled incorrectly.

4) *Applications of Anatomical Labeling in the VBS:* We implemented a function for the automated display of the anatomical name of the bronchial branch in the VBS that we have developed. Fig. 7 shows the presentation of anatomical names in the virtual endoscopic view. Anatomical names of bronchial branches overlapped in the correct position on the endoscopic view. The method selected the currently rendered branches in the virtual endoscopic view and displayed their names. When the user changed the viewpoint and direction of the endoscopic view, the method also selected the corresponding branches. The automated display of branch names was performed smoothly with a frame rate of 6 frames/s on an SGI Octane MXE (CPU:

TABLE II (Continued)

		Total	Level0	Level1	Level2	Level3	Level4	Level5	Level6
Case008	Segmentation	9/19	1/1	2/2	4/4	2/6	0/4	0/2	0/0
	Tree extraction	9	1	2	4	2	0	0	0
	Labeling	9	1	2	4	2	0	0	0
Case009	Segmentation	9/29	1/1	2/2	4/4	2/6	0/6	0/4	0/6
	Tree extraction	9	1	2	4	2	0	0	0
	Labeling	9	1	2	4	2	0	0	0
Case010	Segmentation	23/39	1/1	2/2	4/4	8/9	4/12	4/9	0/2
	Tree extraction	23	1	2	4	8	4	4	0
	Labeling	21	1	2	4	8	4	2	0
Case011	Segmentation	18/40	1/1	2/2	4/4	5/9	6/13	0/9	0/2
	Tree extraction	17	1	2	4	4	6	0	0
	Labeling	11	1	2	4	2	2	0	0
Case012	Segmentation	11/26	1/1	2/2	2/4	4/7	0/8	2/4	0/0
	Tree extraction	9	1	2	2	4	0	0	0
	Labeling	9	1	2	2	4	0	0	0
Case013	Segmentation	25/49	1/1	2/2	4/4	8/9	8/16	2/13	0/4
	Tree extraction	22	1	2	4	7	8	0	0
	Labeling	20	1	2	4	7	6	0	0
Case014	Segmentation	10/47	1/1	2/2	4/4	3/9	0/14	0/11	0/6
	Tree extraction	9	1	2	4	2	0	0	0
	Labeling	9	1	2	4	2	0	0	0
Total	Segmentation	105/249	7/7	14/14	26/28	32/55	18/73	8/52	0/20
	Tree extraction	98	7	14	26	29	18	4	0
	Labeling	88	7	14	26	27	12	2	0
Accumulated	Segmentation	-	7/7	21/21	47/49	79/104	97/177	105/229	105/249
Total	Tree extraction	-	7	21	47	76	94	98	98
	Labeling	-	7	21	47	74	86	88	88

(b)

Levels in Table 2 (a) and (b)	Level1	Level2	Level3	Level4	Level5	Level6
Corresponding anatomical branch names	L. Main Bronchus	L. Upper Lobe Bronchus	R. Middle Lobe Bronchus	RB4	RB7	RB8
	R. Main Bronchus	L. Lower Lobe Bronchus	R. Lower Lobe Bronchus	RB5	LB9	
		R. Upper Lobe Bronchus	L. Superior Division Bronchus	RB6	LB10	
		R. Truncus Intermedius	L. Lingular Bronchus	LB1+2		
			LB6	LB3		
			RB1	LB4		
		RB2	LB5			
		RB3	LB8			

(c)

R10000 250 MHz, main memory: 512 MB). The current branch was defined as the branch satisfying (5). When the user passed through the branching point, the system transiently selected an incorrect branch for a short period of time, but this was not serious. This function proved useful for observing and learning the tree structure of the bronchus and its anatomical name during VBS operation.

## VI. CONCLUSION

We have presented a method for the automated anatomical labeling of a bronchial branch extracted from a 3-D chest CT image and presented applications to the VBS. Experimental results showed that the method segmented 57% of the branches from CT images and extracted the tree structure of 91% of branches in the segmented bronchus. The anatomical labeling

method assigned the correct branch name to 93% of branches in the extracted tree structure. We implemented a function for the automated display of anatomical names of the bronchial branch observed in the virtual endoscopic view. The results showed that the system could overlap the anatomical names of the bronchial branches rendered at the correct position in the endoscopic view.

A careful observation of sample showed that the CT images used in the experiment included more than 500 bronchial branches with different contrasts and a variety of shapes in branching. Therefore, the proposed algorithm was shown to be feasible as the first step in the automated labeling of bronchial branches.

The complete procedure consists of three major steps: bronchus recognition; the tree structure extraction of a given

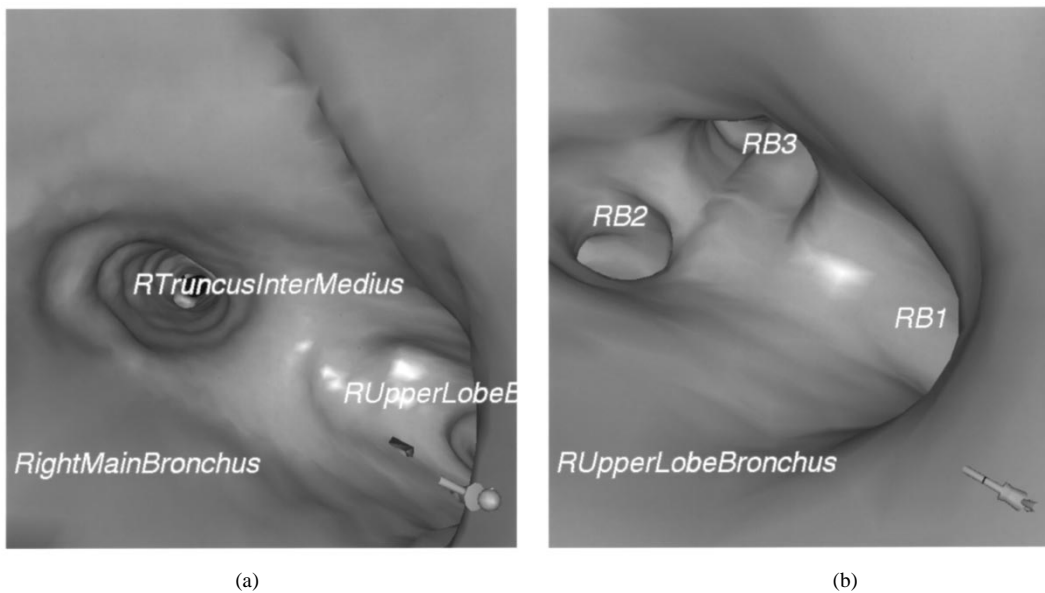


Fig. 7. An example of images of automated display of anatomical names of bronchial branches in VBS. (a) and (b) Rendered at different viewpoints and from different views. Text at left-lower corner shows anatomical name of current branch. Names of child branches of current branch are also automatically presented on virtual endoscopic view.

image; and branch label assignment. Experimental results also revealed several problems in each of these steps that should be solved in the future. The first problem of bronchus recognition has been reported in [14] and included in [6]. Therefore, we briefly note that the spatial resolution of an input image is the important factor. For images of 2.0-mm or smaller slice thickness, the algorithm worked satisfactorily, but the results were worse for those of 5-mm thickness or more. We must improve the 3-D thinning algorithm for the second problem concerning tree structure derivation. In fact, most errors in labeling came from the side effect of the algorithm, such as the generation of a false branch or the loss of a very short branch by degeneration. We must enrich the knowledge base for the third problem concerning tree matching. The proposed method only works in a subset of cases. It cannot correctly treat a case with a different branching structure. The knowledge base used here supports a branching structure where each subsegmental bronchus starts from each segmental bronchus (e.g. RB3a starts from RB3, not RB2). This is because the knowledge base is constructed by considering only one standard type of tree structure of the bronchus, which covers most people in Japan, and additions of other types are desirable. Since the number of samples used in the experiment is limited, the performance evaluation is limited from a statistical viewpoint. Thus, one important problem for a future study is a statistical validation of the result using a larger number of samples.

#### ACKNOWLEDGMENT

The authors would like to thank Dr. K. Katada and Dr. H. Anno of Fujita Health University, Dr. H. Natori of Sapporo Medical University, Dr. M. Mori of Sapporo Kousei Hospital, and Dr. H. Takabatake of Hokkaido Keiai-kai Minami Ichi-jyo Hospital for providing CT images, useful comments, and clinical validation of our system. The authors would also like to thank Mr.

Y.-I. Yoshida for his collaboration in implementing the functions described in Sections III and IV, and colleagues at Nagoya University for useful suggestions and discussions.

#### REFERENCES

- [1] K. Kanazawa, M. Kubo, and N. Niki, "Computer aided diagnosis for lung cancer based on helical CT image," in *Proc. 13th Int. Conf. Pattern Recognition*, vol. III, 1996, pp. 381–3851.
- [2] J. Toriwaki, "Study of computer diagnosis of X-ray and CT images in Japan: A brief survey," in *Proc. IEEE Workshop on Biomedical Image Analysis*, 1994, pp. 155–164.
- [3] J. Toriwaki, "Computerized analysis of chest CT images," in *Proc. 1st Int. Workshop Computer Aided Diagnosis*, 1999, to be published.
- [4] M. Sonaka, W. Park, and E. A. Hoffman, "Rule-based detection of intrathoracic airways trees," *IEEE Trans. Med. Imag.*, vol. 15, pp. 314–326, 1996.
- [5] D. J. Vining, R. Y. Shitrit, and E. F. Haponik *et al.*, "Virtual bronchoscopy," *Radiology*, vol. 193(P), p. 261, 1994.
- [6] K. Mori, J. Hasegawa, J. Toriwaki, H. Anno, and K. Katada, "Automated extraction and visualization of bronchus from 3-D CT images of lung," in *Computer Vision, Virtual Reality and Robotics in Medicine*. ser. Lecture Notes in Computer Science, N. Ayache, Ed. Berlin, Germany: Springer-Verlag, 1995, vol. 905, pp. 542–548.
- [7] R. M. Summers, D. H. Feng, S. M. Holl, M. C. Sneller, and J. H. Shelhamer, "Virtual bronchoscopy: Segmentation method for real-time display," *Radiology*, vol. 200, pp. 857–862, 1996.
- [8] B. Geiger and R. Kikinis, "Simulation of endoscopy," in *Computer Vision, Virtual Reality and Robotics in Medicine*. ser. Lecture Notes in Computer Science, N. Ayache, Ed. Berlin, Germany: Springer-Verlag, 1995, vol. 905, pp. 542–548.
- [9] K. Mori, A. Urano, J. Hasegawa, J. Toriwaki, H. Anno, and K. Katada, "Virtualized endoscope system: An application of virtual reality technology to diagnostic aid," *IEICE Trans. Inform. Syst.*, vol. E79-D, pp. 809–819, 1996.
- [10] G. Rubin, C. Beaulieu, V. Argiro, H. Ringl, A. Norbash, J. Feller, M. Dake, R. Jeffrey, and S. Napel, "Perspective volume rendering of CT and MR images: Applications for endoscopic imaging," *Radiology*, vol. 199, pp. 321–330, 1996.
- [11] C. E. Woodhouse and J. L. Friedman, "In vitro air-contrast-enhanced 3D CT (virtual colonoscopy) appearance of colonic lesions," *Radiology*, vol. 197P, p. 500, 1995.
- [12] K. H. Hoehne, B. Pflesser, A. Pommert, M. Riemer, T. Schiemann, R. Schubert, and U. Tiede, "A virtual body model for surgical education and rehearsal," *Computer*, vol. 29, pp. 25–31, 1996.

- [13] R. Chiplunkar, J. M. Reinhardt, and E. A. Hoffman, "Segmentation and quantization of the primary human airway tree," *Proc. SPIE*, vol. 3033, pp. 403–414, 1997.
- [14] K. Mori, J. Hasegawa, J. Toriwaki, H. Anno, and K. Katada, "Recognition of bronchus in three dimensional X-ray CT images with application to virtualized bronchoscopy system," in *Proc. 13th Int. Conf. Pattern Recognition*, vol. III, 1996, pp. 528–532.
- [15] T. Saito and J. Toriwaki, "A sequential thinning algorithm for three dimensional digital pictures using the Euclidean distance transformation," in *Proc. 8th Scandinavian Conf. Image Analysis*, 1995, pp. 507–516.
- [16] —, "New algorithms for  $n$ -dimensional Euclidean distance transformation," *Pattern Recognit.*, vol. 27, no. 11, pp. 1551–1565, 1994.
- [17] Y. Masutani, T. Schiemann, and K. H. Hoehne, "Vascular shape segmentation and structure extraction using a shape-based region-growing model," in *Medical Image Computing and Computer Aided Intervention*, ser. Lecture Notes on Computer Science. Berlin, Germany: Springer-Verlag, 1998, vol. 1496, pp. 1242–1249.
- [18] N. Chuzo, N. Nagasawa, M. Yamashita, O. Yoshio, and N. Inaba, *The Structure of the Lung, Vol. 1* (in Japanese), ser. The Brochoalveolar System and the Vascular System of the Lung. Tokyo, Japan: Igaku Shoin, 1957.
- [19] S. Ikeda, Ed., *Chest X-Ray Images and Diagnosis* (in Japanese). Tokyo, Japan: Shin Nihon Houki, 1990.
- [20] S. Japan Lung Cancer Society, Ed., *General Rule for Clinical and Pathological Record of Lung Cancer* (in Japanese). Tokyo, Japan: Kanahara Syuppan, 1995.
- [21] P. H. Winston, *Artificial Intelligence*, 3rd ed. Reading, MA: Addison-Wesley, 1992.